JOC Article

Spin Exchange Interaction through Phenylene-Ethynylene Bridge in Diradicals Based on Iminonitroxide and Nitronylnitroxide Radical Derivatives. 1. Experimental Investigation of the Through-Bond Spin Exchange Coupling

Pascale Wautelet,[†,‡,§] Jacques Le Moigne,[‡] Vladimira Videva,[†,||] and Philippe Turek*[,†]

Institut Charles Sadron, UPR 022 CNRS, Université Louis Pasteur, 67083 Strasbourg Cedex, France, Institut de Physique et Chimie des Matériaux de Strasbourg, UMR 7504 CNRS-ULP, 23, rue du Loess, BP 43, 67034 Strasbourg Cedex 2, France, Faculty of Chemistry, Sofia University "St Kliment Ohridski", 1, J. Bourchier Blvd., Sofia 1164, Bulgaria

turek@ics.u-strasbg.fr

Received May 28, 2003

A series of bis-iminonitroxide diradical derivatives of different lengths and geometry have been prepared that incorporate a conjugated phenylene-ethynylene bridge as a rigid spacer. This paper describes the synthesis of these new components and their main characterizations. An unexpected singlet ground state and substituent effects on the singlet−triplet gap have been found for substituted "*m*-phenylene"-based diradicals. The effects of the π-conjugation on the intramolecular through-bond spin coupling have been investigated by changing the length of the spacer within linear derivatives. The EPR studies demonstrate the intramolecular magnetic coupling between the radical spins within all compounds. This result is very attractive and unusual, given the large distance between the radicals from 15 Å in the dimer to 36 Å in the pentamer.

Introduction

An important theme in the design of new magnetic materials[1] is the control of the intramolecular magnetic coupling in organic diradicals and/or polyradicals.[2] The building of diradicals consists of obtaining an exchange interaction between the two spin sites, usually radical centers (R•), through a magnetic coupling unit (MCU) following the Scheme 1a. Different models have been proposed to describe and to predict the ground states of non-Kekulé hydrocarbons.[3] Such rules may serve as a basis for the design of high-spin molecules, but they cannot be extended a priori to heteroatom-containing radicals and couplers. Furthermore, it has often been considered that the molecular conformation plays a decisive role in the spin multiplicity of the ground state.[3e,4] Therefore, the experimental and the theoretical study of the intramolecular magnetic interactions within model systems should be a prerequisite for the evaluation of each coupler/radical system with regard to its MCU ability prior to its use in larger assembly within a given synthetic strategy.

SCHEME 1[a]

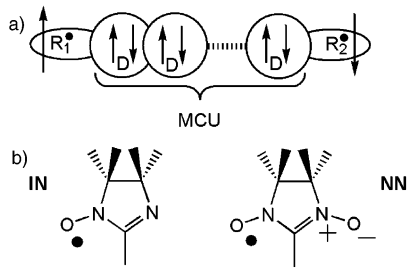

[a] Key: (a) schematic exchange coupling in diradicals; (b) radical fragments for R_1 and R_2.

* To whom correspondence should be addressed. Phone: +33 388 414 000. Fax: +33 388 414 099.
† Université Louis Pasteur.
‡ Institut de Physique et Chimie des Matériaux de Strasbourg.
§ Present address: ExxonMobil Chemical Films Europe, Inc., Virton Plant, Zoning Industriel de Latour, 6761 Virton, Belgium.
|| Sofia University.

(1) (a) Kahn, O. *Molecular Magnetism*; VCH Publishers: New York, 1993. (b) *Molecular Magnetism: From Molecular Assemblies to the Devices*; Coronado, E., Delhaes, P., Gatteschi, D., Miller, J. S., Eds.; Kluwer Academic Publishers: Dordrecht, The Netherlands; 1996; Vol. 321. (c) *Magnetic Properties of Organic Materials*; Lahti, P. M., Ed.; Marcel Dekker: New York, 1999. (d) *Molecular Magnetism-New Magnetic Materials*; Itoh, K., Kinoshita, M., Eds.; Kodansha: Tokyo; Gordon and Breach Science Publishers: Amsterdam, 2000.

(2) For reviews, see: (a) Itoh, K. *Pure Appl. Chem.* **1978**, *50*, 1251. (b) Iwamura, H. *Pure Appl. Chem.* **1986**, *58*, 187; **1987**, *59*, 1595; **1993**, *65*, 57; Iwamura, H. *Adv. Phys. Org. Chem.* **1990**, *26*, 179. (c) Dougherty, D. A. *Acc. Chem. Res.* **1991**, *24*, 88. (d) Iwamura, H.; Koga, N. *Acc. Chem. Res.* **1993**, *26*, 346. (e) Rajca, A. *Chem. Rev.* **1994**, *94*, 871.

(3) (a) Longuet-Higgins, H. C. *J. Chem. Phys.* **1950**, *18*, 265. (b) Mataga, N. *Theor. Chim. Acta* **1968**, *10*, 372. (c) Borden, W. T.; Davidson, E. R. *J. Am. Chem. Soc.* **1977**, *99*, 4587. (d) Ovchinnikov, A. A. *Theor. Chim. Acta* **1978**, *47*, 297. (e) Borden, W. T.; Iwamura, H.; Berson, J. A. *Acc. Chem. Res.* **1994**, *27*, 109.

(4) (a) Dvolaitzky, M.; Chiarelli, R.; Rassat, A. *Angew. Chem., Int. Ed. Engl.* **1992**, *31*, 180. (b) Kanno, F.; Inoue, K.; Koga, N.; Iwamura, H. *J. Am. Chem. Soc.* **1993**, *115*, 847. (c) Silverman, S. K.; Dougherty, D. *J. Phys. Chem.* **1993**, *97*, 13273. (d) Yoshioka, N.; Lahti, P. M.; Takashi, K.; Kuzumaki, Y.; Tsuchida, E.; Nishide, H. *J. Org. Chem.* **1994**, *59*, 4272. (e) Fang, S.; Lee, M. S.; Hrovat, D. A.; Borden, W. T. *J. Am. Chem. Soc.* **1995**, *117*, 6727. (f) Fujita, J.; Tanka, M.; Suemune, H.; Koga, N.; Matsuda, K.; Iwamura, H. *J. Am. Chem. Soc.* **1996**, *118*, 9347. (g) Schultz, D.; Boal, A. K.; Farmer, G. T. *J. Am. Chem. Soc.* **1997**, *119*, 3846.

10.1021/jo034723n CCC: $25.00
Published on Web 09/19/2003

The most ideally considered MCU's are related to phenylene and in particular *m*-phenylene (1,3-diradicals)[2,5] as an expected ferromagnetic coupler between a great variety of radicals. The introduction of a phenylene-based MCU leads to antiferromagnetic (AF) or ferromagnetic (F) exchange coupling depending on the position of the radical substituent (*p*- = 1,4-diradicals, *m*- = 1,3-diradicals, *o*- = 1,2-diradicals), as expected from the "topologically controlled π-spin polarization".[1d,3] The expected triplet magnetic ground state (GS) has been experimentally observed for the *m*-phenylene MCU between nitronylnitroxide radicals (4,4,5,5-tetramethyl-4,5-dihydro-1*H*-imidazol-1-oxyl 3-oxide = **NN**, see Scheme 1b)[6] and for the corresponding iminonitroxide (4,4,5,5-tetramethyl-4,5-dihydro-1*H*-imidazolyl-1-oxyl = **IN**, see Scheme 1b) diradical.[6b]

Among the reported polyradicals, poly(phenylacetylene)s bearing various types of side-chain radical groups have been synthesized,[7] which present a good stability and a high spin concentration. However, the theoretically expected ferromagnetic interactions have not been realized for any of these polymers. Theoretical calculations indicated a nonplanar geometry of the polyene main chain with a preferential cis−transoid conformation.[7f] In addition, the dihedral angle between the backbone and the pendant radical groups is significantly twisted (35−55°). This leads to the inhibition of the cross conjugation in the main chain and to the reduction of the spin density distribution over the polyacetylenic backbone. Poly(*p*-phenylene)s and poly(phenylene-vinylene)s could be other possible candidates for developing magnetic polyradicals. Poly(*p*-phenylene)s present a good solubility but the proximity of the neighboring phenylene rings induces a steric hindrance between the substituents or the hydrogens in the ortho position of the phenyl groups. This steric hindrance is minimized by rotations about the simple bond, leading to the deviation from coplanarity of the main chain and, hence, the decrease of the conjugation pathway. Moreover, it has been considered as being responsible for the twist of the radical substituent with respect to the main chain.[8] Various stilbenoid diradicals including oligo(1,2-phenylene-vinylene) as spacers have been shown to exhibit the intramolecular through-bond ferromagnetic coupling.[9a−c] The subsequently synthesized poly(phenylene-vinylene) polyradical derivatives have been recently reported to exhibit the intramolecular ferromagnetic coupling.[9d−h] Parallel to these works, the phenylene-ethynylene unit could be guessed for its higher chain rigidity and π-conjugation. The *m*-phenylene-ethynylene bridge as an MCU has been shown to be quiet inefficient in most cases,[10c−h] except for triplet spins nitrenophenyl radicals.[10a,b] The exchange coupling through *m*-phenylene-ethynylene is weak in diradicals and related polyradicals bearing various pendant radicals, including **NN**. The spin multiplicity of the magnetic GS is not well assessed, since most studies point at possible nearly vanishing singlet−triplet (ST) splitting.

The lack of the observation of strong magnetic coupling in poly(phenylene-ethynylene) as compared to poly(phenylene-vinylene) requires a better understanding of the mechanisms of the through-bond spin coupling. Such studies should also be of valuable interest with respect to the growing field of photomagnetism in molecular magnetic materials.[1c,d] The present study is focusing on the synthesis of a series of diradicals, which are based on **IN** and/or **NN** terminal radical subunits connected through a diamagnetic conjugated organic spacer, the phenylene-ethynylene oligomers. The physicochemical characterization of all synthesized molecules including their magnetic properties (SQUID, EPR) is fully documented.[11]

A parallel theoretical study has been performed on the molecules synthesized and characterized in the present experimental work, extending the work to higher oligomers and MCUs and considering the effects of molecular conformation in related derivatives.[11d] The results of this theoretical investigation will be detailed in a forthcoming publication, hereafter designated as part 2.

Results and Discussion

Synthesis. The general synthetic scheme for the diradicals derivatives of **IN** and **NN** is based on a palladium-catalyzed cross-coupling reaction derived from

(5) Recent reports: (a) Shultz, D. A.; Boal, A. K.; Farmer, G. T. *J. Org. Chem.* **1998**, *63*, 9462. (b) Fico, R. M.; Hay, M. F.; Reese, S.; Hammond, S.; Lambert, E.; Fox, M. A. *J. Org. Chem.* **1999**, *64*, 9386. (c) Adam, W.; Baumgarten, M.; Maas, W. *J. Am. Chem. Soc.* **2000**, *122*, 6735. (d) Domingo, V. M.; Aleman, C.; Brillas, E.; Juliá, L. *J. Org. Chem.* **2001**, *66*, 4058. (e) Shultz, D. A.; Bodnar, S. H.; Lee H.; Kampf, J. W.; Incarvito, C. D.; Rheingold, A. L. *J. Am. Chem. Soc.* **2002**, *124*, 100547. (f) Dei, A.; Gatteschi, D.; Sangregorio, C.; Sorace, L.; Vaz, M. G. F. *Inorg. Chem.* **2003**, *42*, 1701.

(6) (a) Shiomi, D.; Tamura, M.; Sawa, H.; Kato, R.; Kinoshita, M. *J. Phys. Soc. Jpn.* **1993**, *62*, 289. (b) Catala, L.; Le Moigne, J.; Kyritsakas, N.; Rey, P.; Novoa, J.-J.; Turek, P. *Chem. Eur. J.* **2001**, *7*, 2466. (c) Catala, L. Doctoral Thesis, University of Strasbourg, France, 1999. (d) Catala, L. et al. To be published.

(7) (a) Nishide, H.; Yoshioka, N.; Inagaki, K.; Tsuchida, E. *Macromolecules* **1988**, *4*, 3119. (b) Fujii, A.; Ishida, T.; Koga, N.; Iwamura, H. *Macromolecules* **1991**, *24*, 1077. (c) Yoshioka, N.; Nishide, H.; Kaneko, T.; Yoshiki, H.; Tsuchida, E. *Macromolecules* **1992**, *25*, 3838. (d) Miura, Y.; Inui, K.; Yamaguchi, F.; Inoue, M.; Teki, Y.; Takui, T.; Itoh, K. *J. Polym. Sci., Polym. Chem. Ed.* **1992**, *30*, 959. (e) Miura, Y.; Matsumoto, M.; Ushitani, Y.; Nishide, H.; Kaneko, T.; Igarashi, M.; Teki, Y.; Takui, T.; Itoh, K. *Macromolecules* **1993**, *26*, 6673. (f) Tsuchida, E.; Yoshioka, N.; Lahti, P. M. *Macromolecules* **1994**, *27*, 3082.

(8) Oka, H.; Tamura, T.; Miura, Y.; Teki, Y. *J. Mater. Chem.* **1999**, *9*, 1227.

(9) (a) Yoshioka, N.; Lahti, P. M.; Kaneko, T.; Kuzumaki, Y.; Tsuchida, E.; Nishide, H. *J. Org. Chem.*, **1994**, *59*, 4272. (b) Kaneko, T.; Toriu, S.; Tsuchida, E.; Nishide, H.; Yamaki, D.; Maruta, G.; Yamaguchi, K. *Chem. Lett.* **1995**, 421. (c) Maruta, G.; Yamaki, D.; Mori, W.; Yamaguchi, K.; Nishide, H. *Mol. Cryst. Liq. Cryst.* **1996**, *279*, 19. (d) Nishide, H.; Kaneko, T.; Nii, T.; Katoh, K.; Tsuchida, E.; Yamaguchi, K. *J. Am. Chem. Soc.* **1995**, *117*, 548. (e) Nishide, H.; Kaneko, T.; Toriu, S.; Kuzumaki, Y.; Tsuchida, E. *Bull. Chem. Soc. Jpn.* **1996**, *69*, 499. (f) Nishide, H.; Kaneko, T.; Nii, T.; Katoh, K.; Tsuchida, E.; Lahti, P. M. *J. Am. Chem. Soc.* **1996**, *118*, 9695. (g) Nishide, H.; Miyasaka, M.; Tsuchida, E. *J. Org. Chem.* **1998**, *63*, 7399. (h) Nishide, H.; Ozawa, T.; Miyasaka, M.; Tsuchida, E. *J. Am. Chem. Soc.* **2001**, *123*, 5942.

(10) (a) Murata, S.; Iwamura, H. *J. Am. Chem. Soc.* **1991**, *113*, 5547. (b) Sasaki, S.; Iwamura, H. *Chem. Lett.* **1992**, 1759. (c) Swoboda, P.; Saf, R.; Hummel, K.; Hofer, F.; Czaputa, R. *Macromolecules* **1995**, *28*, 4255. (d) Saf, R.; Swoboda, P.; Lechner, A.; Hummel, K.; Czaputa, R. *Macromol. Chem. Phys.* **1996**, *197*, 1439. (e) Miura, Y.; Issiki, T.; Ushitani, Y.; Teki, Y.; Itoh, K. *J. Mater. Chem.* **1996**, *6*, 1745. (f) Schultz, D. A.; Lee, H.; Kumar, R. K.; Gwaltney, K. P. *J. Org. Chem.* **1999**, *64*, 9124. (g) Van Meurs, P. J.; Janssen, R. A. J. *J. Org. Chem.* **2000**, *65*, 5712. (h) Akita, T.; Koga, N. *Polyhedron* **2001**, *20*, 1475.

(11) Part of the results have been preliminarily published as conference proceedings, and a thesis has been defended: (a) Turek, P.; Wautelet, P.; Le Moigne, J.; Stanger, J.-L.; André, J.-J.; Bieber, A.; Rey, P.; De Cian, A.; Fisher, J. *Mol. Cryst. Liq. Cryst* **1995**, *272*, 99. (b) Wautelet, P. Doctoral Thesis, University of Strasbourg, France, 1996. (c) Wautelet, P.; Bieber, A.; Turek, P.; Le Moigne, J.; André, J.-J. *Mol. Cryst. Liq. Cryst.* **1997**, *305*, 55. (d) Wautelet, P.; Bieber, A.; Catala, L.; Turek, P.; Le Moigne, J.; André, J.-J. *Polyhedron* **2001**, *20*, 1571.

SCHEME 2. Chemical Structure of Mono- and Diradicals Studied Experimentally in the Present Work

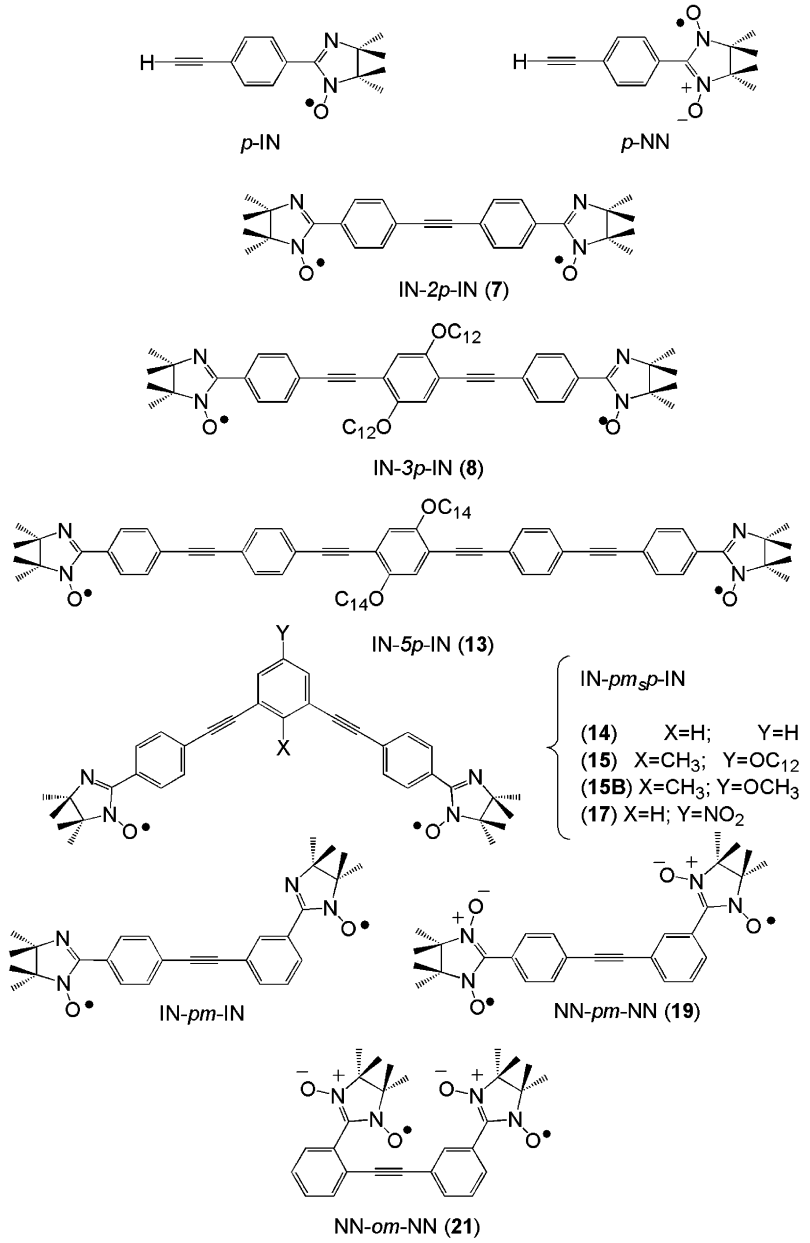

the Heck−Sonogashira coupling between an ethynylarene and a halogenoaryl compound. Scheme 3 shows the chemical route to prepare the desired diradical dimers **IN-*2p*-IN (7)** and **NN-*pm*-NN (19)**. The 4-bromobenzaldehyde **(1)** was first reacted with a palladium complex **(i)** in the presence of trimethylsilylacetylene (TMSA) **(ii)** in triethylamine to give the intermediate **3**. Compound **3** was then treated with K_2CO_3 in methanol at room temperature to give the 4-ethynylbenzaldehyde **(4).** Both aldehydes **1** and **4** were coupled separately with 2,3-bis-(hydroxyamino)-2,3-dimethylbutane **(2)** in methanol to give, respectively, the imidazoline derivatives **5** and **6**. These derivatives were prepared basically by following the route given in the literature.[12−14] Slight modifications to the procedure described to obtain **2**[14] afforded higher yield (see the Experimental Section). Oxidation of **6**[15] with manganese oxide **(iii)** in dichloromethane gave the corresponding nitronyl-nitroxide ***p*-NN** (Scheme 2) derivative from which the iminonitroxide radical ***p*-IN** (Scheme 2) was obtained by treatment with sodium nitrite and hydrochloric acid.[16] The condensation of imidazolines **5** and **6** catalyzed by the palladium complex **i** in triethylamine gave directly the iminonitroxide precursor **7′** avoiding a mixture of iminonitroxide and nitronylnitroxide. The diradical **IN-*2p*-IN** (**7**) was obtained from **7′** by reaction with manganese oxide in dichloromethane.

(12) Osiecki, J. H.; Ullman, E. F. *J. Am. Chem. Soc.* **1968**, *90*, 1078.
(13) Sayre, R. *J. Am. Chem. Soc.* **1955**, *77*, 6689.
(14) Lamchen, M.; Mittag, T. W. *J. Chem. Soc. C* **1966**, 2300.
(15) Ullman, E. F.; Osiecki, J. H.; Boocock, D. G. B.; Darcy, R. *J. Am. Chem. Soc.* **1972**, *94*, 7049.
(16) Rey, P.; Luneau, D. In *Supramolecular Engineering of Synthetic Metallic Materials*: *Conductors and Magnets*; Veciana, J., Rovira, C., Amabilino, D. B., Eds.; NATO ASI Ser., Ser. C; Kluwer Academic Publishers: Dordrecht, 1999; Vol. 518, p 145.

SCHEME 3. General Route for the Synthesis of IN and NN Diradicals: Synthesis of 7 and 19[a]

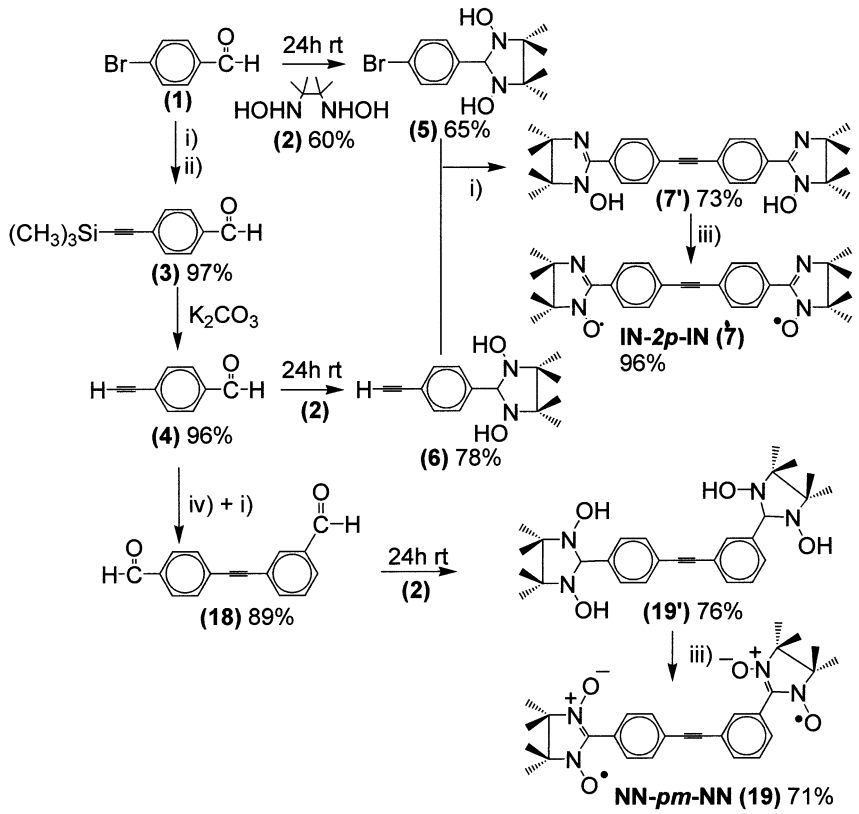

[a] Key: (i) $PdCl_2$−TPP−$Cu(OAc)_2$; (ii) TMSA; (iii) MnO_2; (iv) 3-bromobenzaldehyde.

The trimers **IN-*3p*-IN** (**8**), **IN-*pmp*-IN** (X = H, Y = H) (**14**), **IN-*pm*$_S$*p*-IN** (X = CH_3, Y = OC_{12}) (**15**), **IN-*pm*$_S$*p*-IN** (X = CH_3, Y = OCH_3) (**15B**), and **IN-*pm*$_S$*p*-IN** (X = H, Y = NO_2) (**17**) were obtained similarly by the condensation of 2 equiv of the terminal ethynylimidazoline **(6)** with 1 equiv of the corresponding dibromobenzene derivatives.[17] Slight modifications of the procedure described to obtain the iminonitroxyl derivatives were used to generate pure nitronylnitroxide diradicals **NN-*pm*-NN** (**19**) and **NN-*om*-NN** (**21**). The first step was the preparation of the di(formylphenyl)ethyne derivatives **18** and **20**, from which the resulting di(bis(hydroxyamines)) **19′** and **21′** were obtained by reaction with 2,3-bis(hydroxyamino)-2,3-dimethylbutane (**2**) in methanol. The oxidation of these compounds gave exclusively the **NN-*pm*-NN** and **NN-*om*-NN** diradicals.

The most interesting aspect of the synthetic strategy was the generation of the longest oligomer of this series, the pentamer **IN-*5p*-IN**. It was synthesized step by step by a selective protection and deprotection method previously described in the literature.[17] The general procedure is shown in Scheme 4. 4-Bromoaniline was protected on each side by trimethylsilyl and triazene groups, respectively, to give **10**. The triazene group was then removed by treatment of **10** with methyl iodide, affording the monoprotected derivative **11**. Condensation of **11** with the imidazoline **6**, catalyzed by the palladium complex **i** in triethylamine, gave the intermediate **12′** from which the deprotected dimer **12** was obtained by reaction with tetrabutylamonium fluoride in tetrahydrofuran. The catalyzed condensation of **12** and 1,4-dibromo-2,6-bis-(tetradecanoxy)benzene[15] afforded the pentamer **13′**. Careful oxidation of **13′** with manganese oxide gave the diradical **IN-*5p*-IN** (**13**) in high yield.

Purity and Characterization. The chemical purities of the intermediates in the synthetic routes were investigated by elemental analysis and ^{1}H NMR. The relevant results of these studies are given in the Experimental Section. The final products were subjected to several recrystallizations from heptane−dichloromethane solution to give, by slow evaporation, dark red (**IN**) or dark blue (**NN**) crystals. The elemental analysis (C, H, O, N) were performed for all compounds and found to be within acceptable uncertainties (± 0.4%) as indicated in the Experimental Section. Their chemical structures were confirmed by infrared, UV−vis, and EPR spectroscopy.

The number of spins 1/2 per molecule, n_s, is reported in Table 1 for the various compounds. It was determined by integration of the EPR signal calibrated against a standard (VARIAN pitch) in the solid state at room temperature. It is well-known that spin calibration by EPR suffers from various imperfections, e.g., numerical errors arising from double integration (baseline correction), comparison with a standard sample without being able to use the same spectrometer conditions, and electrostatic powders attached along the sample tube, therefore yielding an underestimate of the sample weight. When such measurements are available as in most cases in the present work, it is more accurate to estimate n_s from the Curie constant given by the static spin suscep-

(17) Wautelet, P.; Moroni, M.; Oswald, L.; Le Moigne, J.; Pham, A.; Bigot, J.-Y. *Macromolecules* **1996**, *29*, 446.

SCHEME 4. Route for the Synthesis of Compound IN-*5p*-IN[a]

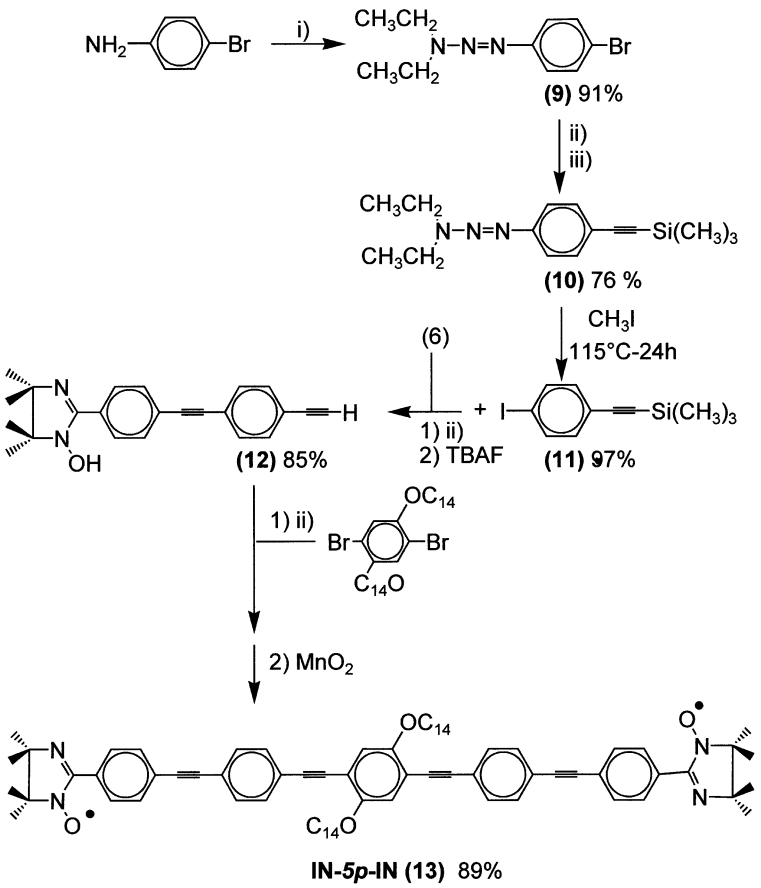

[a] Key: (i) (1) $HCl/NaNO_2$, (2) NEt_2/K_2CO_3; (ii) $PdCl_2-TTP-Cu(OAc)_2$; (iii) TMSA.

TABLE 1. Spin 1/2 Concentration per Molecule for the Various Radical Compounds As Deduced from Spin Calibration Measurements (Curie Constant from SQUID or EPR Spin Calibration)

	n_s
***p*-NN**	0.8[a]
***p*-IN**	1.09
IN-*2p*-IN	2.1[a]
IN-*3p*-IN	1.99
IN-*5p*-IN	1.9
IN-*pmp*-IN	1.5
IN-*pm*$_S$*p*-IN X = CH_3; Y = OC_{12}	1.95
IN-*pm*$_S$*p*-IN X = H; Y = NO_2	1.97
IN-*pm*-IN	1.80
NN-*pm*-NN	1.80
NN-*om*-NN	1.7[a]

[a] EPR spin calibration.

tibility as determined by a SQUID susceptometer. It is concluded from these estimations, that the obtained molecules may be considered as monoradicals or diradicals in agreement with the synthesis objectives, except for **IN-*pmp*-IN**.

For all studied polycrystalline materials, the susceptibility data obtained from SQUID susceptometer follow Curie−Weiss-like behaviors ($\chi = C/T - \theta$), with the Curie constant, C, and the mean-field temperature, θ. For all studied compounds but ***p*-IN** ($\theta = +1$ K), θ is negative in the range (−2 K, 0 K). It indicates a weak antiferromagnetic exchange correlation in these polycrystalline materials. It is worth noting that the mean field temperature reported for a crystalline sample cannot be considered as an estimation of the intramolecular magnetic coupling. Except for the peculiar case of isolated molecules within a given crystal lattice, this may hardly occur. The discussion of the possible intermolecular magnetic interactions within the crystalline state[18] is out of the scope of the present work.

Optical Properties. We have reported in Table 2 the relevant results of the UV−vis, infrared, and Raman scattering spectroscopies.

The IR spectra of the radical oligomers clearly indicate a complete disappearance of the stretching vibration of the O−H bond, which is characteristic of the hydroxy precursors, while a sharp band around 1460 cm^{-1}, attributed to the NO• radical, appears after oxidation.

The UV−vis absorption spectra of the radicals also present a sharp absorption around 548 nm for IN derivatives and 610 nm for NN derivatives. This absorption band is assigned to the N−O group.

The absorption spectra of the linear diradicals **IN-(*xp*)-IN** ($x = 2, 3, 5$) in dichloromethane are given in Figure 1. The **IN-*2p*-IN** spectrum presents a main peak in the

(18) Single crystals were obtained for the ***p*-NN**, ***p*-IN**, **IN-*pm*$_S$*p*-IN** (X = H; Y = OC_{12}), and **IN-*3p*-IN** compounds. The X-rays crystal structures were determined with a good refinement for the ***p*-IN** and the ***p*-NN** materials, whereas some disorder was observed in the case of **IN-*pm*$_S$*p*-IN** (X = H; Y = OC_{12}). See ref 11b.

TABLE 2. Spectroscopic Data of the Various Mono- and Diradicals Based on IN and NN in Solutions or Dispersed in KBr Pellets

	UV−vis		IR	Raman
mono- and diradicals	λ (nm) solution[a]	$\epsilon \times 10^2$ (L·mol^{-1}·cm^{-1}) solution[a]	$\nu_{C\equiv C}$ (cm^{-1}) KBr pellets	$\nu_{C\equiv C}$ (cm^{-1}) solution
***p*-NN**	318, 605*	347, 7.8	2098	
***p*-IN**	262, 457	273, 5.6	2099	
IN-*2p*-IN	314, 457	356, 10	2210	2239
IN-*3p*-IN	320, 383, 458*	520,480, 19	2207	2236
IN-*5p*-IN	337, 390, 459*	825, 878, 20	2203	2234
IN-*pmp*-IN	302, 459	646, 10	2210	2241
IN-*pm*$_s$p-IN X=CH$_3$;Y=OC$_{12}$	302, 460	1000, 13	2211	2241
IN-*pm*$_s$p-IN X=H; Y=NO$_2$	305, 462	688, 14	2209	2240
IN-*pm*-IN	300, 457	348, 10	2210	2239
NN-*pm*-NN	315, 609	348, 5.2		2240
NN-*om*-NN	314, 608	351, 5.6		

[a] The underlined values are relative to the **IN** or **NN** radicals and the wavelengths with asterisks correspond to shoulders.

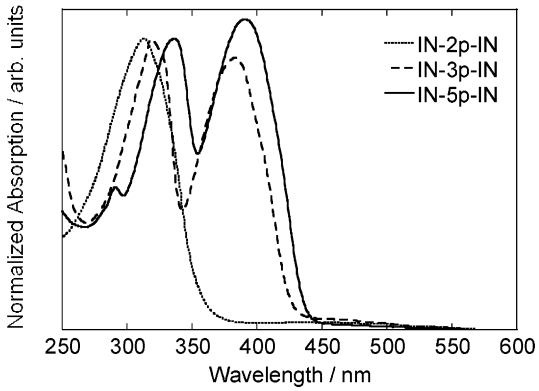

FIGURE 1. UV−vis optical spectra of **IN-*2p*-IN**, **IN-*3p*-IN**, and **IN-*5p*-IN** in solution in CH_2Cl_2.

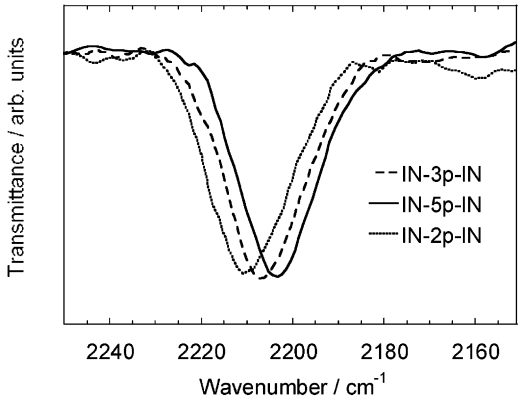

FIGURE 2. Infrared spectra of **IN-*2p*-IN**, **IN-*3p*-IN**, and **IN-*5p*-IN** in solid-state KBr pellets.

near-UV with a maximum centered at $\lambda = 314$ nm ($\epsilon = 3.6 \times 10^4$ L·mol^{-1}·cm^{-1}), due to $\pi-\pi^*$ transition and a very weak absorption in the visible at $\lambda = 457$ nm ($\epsilon = 1.0 \times 10^2$ L·mol^{-1}·cm^{-1}), corresponding to n$-\pi^*$ transition in NO•.[15] The diradicals **IN-*3p*-IN** and **IN-*5p*-IN,** which have lateral donors in the side chains O−R, are slightly different from **IN-*2p*-IN.**

They show two intense absorption bands in the near UV−vis at 320 ($\epsilon = 5.2 \times 10^4$ L·mol^{-1}·cm^{-1}) and 383 nm ($\epsilon = 4.8 \times 10^4$ L·mol^{-1}·cm^{-1}), at 337 ($\epsilon = 8.2 \times 10^4$ L·mol^{-1}·cm^{-1}) and 390 nm ($\epsilon = 8.8 \times 10^4$ L·mol^{-1}·cm^{-1}) for **IN-*3p*-IN** and **IN-*5p*-IN**, respectively. The UV bands correspond to the $\pi-\pi^*$ transition also observed for **IN-*2p*-IN**, and the additive band observed for the **IN-*3p*-IN** and **IN-*5p*-IN** can be attributed to the internal charge transfer due to the donor substituents. The intramolecular charge transfer is well-known for phenyl derivatives,[19] and a donor gives a very efficient charge transfer to the conjugated chain through the phenyl ring. The spectra also show very weak absorptions in the range 450−600 nm (as shoulders), due to NO• as observed in **IN-*2p*-IN** ($\lambda_{max} \sim 457$ nm). The most interesting result is the red shift of the absorption bands between the dimer and the trimer and also between the trimer and the pentamer, showing the dependency of the absorption wavelengths with the chain length. This red shift of wavelengths is associated with the increase of the π-electron delocalization along the linear phenyl-ethynyl chain.[20]

The "broken chain" derivatives **IN-*pm*-IN** and **IN-*pmp*-IN** show almost similar features on their spectra, with a main band centered at 300−305 nm, indicating no influence of the substituents on the conjugation of the chain. The Raman scattering of the vibrational modes of the unsaturated bonds is a sensitive method for the characterization of π-electron delocalization in unsaturated molecules. The normal modes associated with the triple bond stretching in a phenyl-ethynyl derivative are observed around 2210 cm^{-1}. Figures 2 and 3 show the C≡C stretching band of **IN-(*xp*)-IN** ($x = 2, 3, 5$) samples by infrared in the solid-state KBr pellets and by Raman on mixed solution (xylene/dichloromethane), respectively. A shift to lower frequencies is found, going from the dimer ($\nu_{IR} = 2210$ cm^{-1}; $\nu_{Raman} = 2239$ cm^{-1}) to the trimer ($\nu_{IR} = 2207$ cm^{-1}; $\nu_{Raman} = 2236$ cm^{-1}) and from the trimer to the pentamer ($\nu_{IR} = 2203$ cm^{-1}; $\nu_{Raman} = 2234$ cm^{-1}). These shifts in the pentamer and in the trimer (related to the dimer) are due to an increase of the π-electron delocalization along the conjugated backbone, which have

(19) Moroni, M.; Le Moigne, J.; Luzzati, S. *Macromolecules* **1994**, *27*, 562.

(20) Schumm, J. S.; Pearson, D. L.; Tour, J. M. *Angew. Chem., Int. Ed. Engl.* **1994**, *33*, 1360.

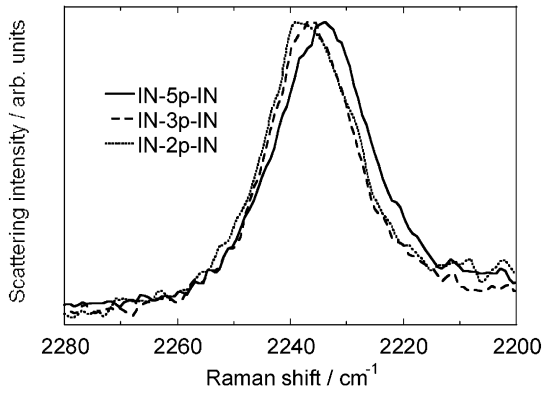

FIGURE 3. Raman scattering spectra of **IN-*2p*-IN**, **IN-*3p*-IN**, and **IN-*5p*-IN** in solution in CH_2Cl_2/xylene 1/1.

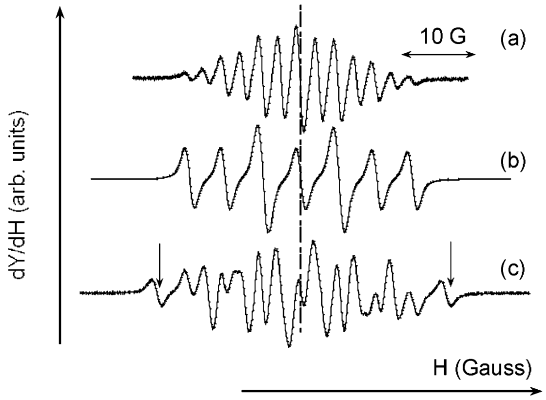

FIGURE 4. EPR spectrum of the linear diradical derivatives: (a) **IN-*2p*-IN** (**7**), (b) ***p*-IN**, and (c) **IN-*5p*-IN** (**13**). The arrows in (c) show the appearance of outer extra-lines compared to (a).

been also detected in the UV−vis absorption spectra. The triple-bond stretching for the broken chain derivatives **IN-*pm*-IN** and **IN-*pm*$_S$p-IN** are observed around 2210 cm^{-1} for the trimer in agreement with the UV−vis results.

Fluid-Solution EPR Spectroscopy. The EPR spectra of the different radical derivatives have been recorded at room temperature in a degassed 1:1 mixed solution of CH_2Cl_2/xylene in order to avoid the aggregates observed in various solvents. The typical concentrations for the room-temperature studies are in the range 10^{-5}−10^{-4} M. The spectrum of ***p*-IN** (Figure 4b) exhibits the typical seven-line hyperfine pattern of an imino nitroxide radical.[15] The hyperfine coupling constants (hfcc's) for the two unequivalent ^{14}N nuclei (a_{N1}, a_{N2}) are estimated from the simulated spectrum as $a_{N1} = 9.10$ G; $a_{N2} = 4.22$ G, with the individual Gaussian line width $\Delta B_{pp} = 1.12$ G and the *g*-factor $g = 2.0059$. The room-temperature spectra of the diradicals are different from the above-described monoradical spectrum (Figure 4a,c).

The radical spins within the **IN-*2p*-IN** (Figure 4a) diradical must be described as interacting within the strong exchange limit $|J| \gg |a_N|$, where *J* is the intramolecular exchange interaction and a_N is the hyperfine interaction.[21] The same observations hold for **IN-*3p*-IN**. It results in the pairing of the two nonequivalent ^{14}N nuclei on each side of the diradical yielding half values

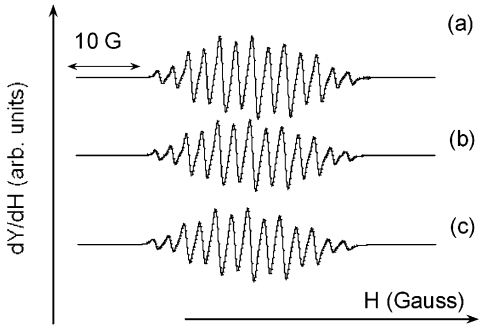

FIGURE 5. EPR spectrum of the *m*-phenylene-based diradicals: (a) **IN-*pmp*-IN (14)**, (b) **IN-*pm*$_S$*p*-IN** (X = H, Y = NO_2) (**17**), and **IN-*pm*$_S$*p*-IN** (X = CH_3, Y = OC_{12}) (**15**).

for the hfcc's as compared to the monoradical ones; e.g., the simulated spectrum of **IN-*3p*-IN** affords the following estimations of the hfcc's by spectrum simulation, $a_{N1} = 4.53$ G; $a_{N2} = 2.22$ G with $\Delta B_{pp} = 0.85$ G and $g = 2.0059$. This observation is very attractive, since one would expect the isolated spins in these diradicals where the distance between radicals is very large (15 and 21 Å).[22] The situation appears more complicated in the case of the **IN-*5p*-IN** compound (Figure 4c). As compared to the monoradical and to the other diradicals, the spectrum is strongly distorted and additional lines are observed. This is interpreted as indicating the limit of intermediate exchange, i.e., as the exchange interaction is of the order of magnitude of the hyperfine interaction.[23] The outer extra lines may be attributed to singlet transitions (S resonances indicated by arrows on Figure 4), although these are not as strongly attenuated with respect to the principal components as reported in the literature.[23d,e] This assumption affords an estimation of the exchange interaction as being larger than a few mK, i.e., a few hfcc's. The decrease of the strength of the exchange interaction is quite expected in the present series of linear oligomers as the interspin distance increases. Moreover, the pentamer **IN-*5p*-IN** does appear as being close to the limiting distance for the exchange to be observed. The through-bond pathway for the spin exchange interaction must be considered up to ca. 40 Å in these rigid rodlike molecules studied in diluted solutions. It is worth noting the recent demonstration of the through bond dipolar coupling up to 20 Å between nitroxide radicals connected through a rigid and conjugated chain close to the one studied in the present work.[24]

The substituted diradical derivatives based on *m*-phenylene have been studied under the same conditions as described above for the linear derivatives. The EPR spectra recorded at room temperature (Figure 5) are similar to those of the linear diradicals (see Figure 4),

(21) (a) Luckhurst, G. R. In *Spin Labeling. Theory and applications*; Berliner, J. L., Ed.; Academic Press: New York, 1976; p 133 ff. (b) Luckhurst, G. R.; Pedulli, G. F. *J. Am. Chem. Soc.* **1970**, *92*, 4738.

(22) (a) McConnell, H. M. *J. Chem. Phys.* **1960**, *33*, 115−121. (b) Lahti, P. M.; Ichimura, A. S. *J. Org. Chem.* **1991**, *56*, 3031.

(23) (a) Hernandez-Gasiò, E.; Mas, M.; Molins, E.; Rovira, C.; Veciana, J.; Borrasalmenar, J. J.; Coronado, E. *Chem. Mater.* **1994**, *6*, 2398. (b) Hernandez-Gasiò, E. Ph.D. Thesis, University of Barcelona, Spain, 1993. (c) Brière, R.; Dupeyre, R.-M.; Lemaire, H.; Morat, C.; Rassat, A.; Rey, P. *Bull. Soc. Chim. Fr.* **1965**, 3290. (d) Metzner, K. E.; Libertini, L. J.; Calvin, M. *J. Am. Chem. Soc.* **1977**, *99*, 4500. (e) Glarum, S. H.; Marshall, J. H. *J. Chem. Phys.* **1967**, *47*, 1374.

(24) Jeschke, G.; Pannier, M.; Godt, A.; Spiess, H. W. *Chem. Phys. Lett.* **2000**, *331*, 243.

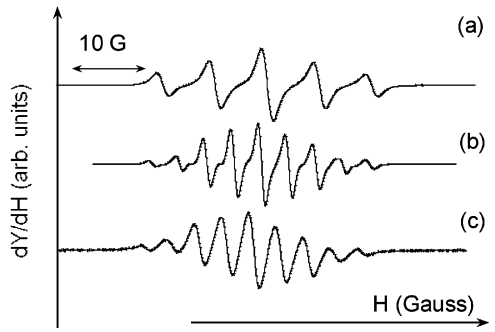

FIGURE 6. EPR spectrum of the nitronyl nitroxide derivatives: (a) ***p*-NN**, (b) **NN-*pm*-NN** (**19**), and (c) **NN-*om*-NN** (**21**).

except for the broadening of the hyperfine lines at high field. The asymmetry is due to the slowing down of the molecular tumbling.[21,25] It is concluded that the three diradicals must be considered within the strong exchange limit.

The EPR spectra of the nitronylnitroxide diradical derivatives exhibit the nine-line hyperfine pattern expected in the limit of the strong exchange coupling resulting in four equivalent ^{14}N nuclei (Figure 6). The broadening of the individual lines in the case of **NN-*om*-NN** (Figure 6c) is attributed to the direct through-space interaction (exchange and/or dipolar).

It is worth noting that the EPR spectra of all synthesized compounds exhibit the expected hyperfine pattern. This should be considered as a valuable support for their chemical purity.[26] For instance, the apparent spin deficit for **IN-*pmp*-IN** would be easily detected if it resulted from a mixture of a monoradical and a diradical with a measurable concentration of monoradical. Although the incomplete oxidation may occur, it does not produce preferentially such a mixture. Also, it is worth noting that the lack of the observation of obvious traces of monoradical in **IN-*pm*-IN** supports the experiments in frozen solution presented in the next section, since the presence of monoradical (if any) is not expected to strongly disturb the observed signal of the diradical.

Frozen-Solution EPR Spectroscopy: Determination of the Magnetic Ground State and of the Singlet−Triplet Splitting. Neither the sign nor the strength of the intramolecular exchange interaction can be inferred from the previous studies at room temperature. These have been determined for the frozen solutions upon studying the temperature dependence (4−100 K) of the doubly integrated EPR absorption signals or EPR susceptibility, χ_{EPR}, recorded in the $\Delta M_S = 1$ region. The frozen solutions were obtained upon cooling the previously described fluid solutions. In some cases (**IN-*2p*-IN** and **IN-*pmp*-IN**), a diluted solution of the compound was mixed within a polystyrene polymer matrix, followed by lyophilization in a benzene solution. The lack of the formation of molecular aggregates was deduced from the reversible observation of the high-temperature solution spectra upon going up and down through the melting point of the solutions (ca. 170 K). The EPR spectra of the compounds in frozen glassy matrix appear as slightly

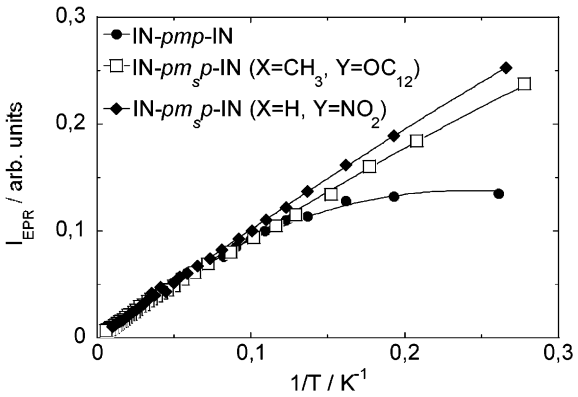

FIGURE 7. EPR-integrated intensity as a function of the reciprocal temperature for **IN-*pm*$_s$*p*-IN** derivatives **14**, **15**, and **17**. Continuous lines are the fit with a dimer model (eq 1).

distorted and weakly or not structured, with ΔB_{pp} of the order of 10−20 G. Fine structure lines could not be assigned in the present series of derivatives. This is well understood, since the large distance between the spin sites yields very small zero-field splitting. Related to this argument, a half-field signal corresponding to the $\Delta M_S = 2$ transitions was not observed.[27] Care was taken against possible microwave saturation effects, which may occur in particular at low temperature (see the Experimental Section). The temperature dependence of the EPR susceptibility is close to linear Curie plots (χ_{EPR} vs $1/T$) for all of the compounds. As reported in previous works,[2e,3e,28] a linear Curie plot means either a large ferromagnetic interaction yielding the triplet ground state (GS) or a small energy gap of the order kT between nearly degenerate singlet and triplet states, hence a possible singlet GS. In the latter case, the singlet GS will be deduced from the observation of a downward curvature of the χ_{EPR} vs $1/T$ plot at low temperature.

The susceptibility data have been fitted by a Bleaney−Bowers expression[29]

$$\chi = \frac{C}{T}\frac{3}{3 + \exp(-T_{ST}/T)} \qquad (1)$$

where C is a constant to fit the sample intensity and T_{ST} is the characteristic intramolecular exchange temperature defining the ST energy gap. The positive T_{ST} indicates the triplet GS, whereas the negative ones points to the singlet GS.

A typical Curie plot of χ_{EPR} is shown in Figure 7 for the three ***pm*$_s$*p*** derivatives. The downward deviations from the linear plot are observed for the three derivatives with the largest one for the nonsubstituted derivative, **IN-*pmp*-IN**. The results of the fits are given in Table 3 for all compounds.

The intramolecular antiferromagnetic exchange coupling yielding the singlet GS is estimated for all compounds. For ***pm*** and ***om*** geometries, the sole indication of a magnetic coupling is the observation of the diradical

(25) (a) Luckhurst, G. R.; Pedulli, G. F. *Mol. Phys.* **1971**, *20*, 1043. (b) Alster, E.; Silver, B. L. *Mol. Phys.* **1986**, *58*, 977.

(26) Shultz, D. A.; Boal, A. K.; Lee, H.; Farmer, G. T. *J. Org. Chem.* **1999**, *64*, 4386: see Table 1 of this paper.

(27) Weissman, S. I.; Kothe, G. *J. Am. Chem. Soc.* **1975**, *97*, 2537.

(28) (a) Berson, J. A. In *The Chemistry of the Quinonoid Compounds*; Patai, S., Rappoport, Z., Eds.; Wiley: New York, 1988; Vol. II, p 482. (b) Matsuda, K.; Iwamura, H. *J. Chem. Soc., Perkin Trans. 2* **1998**, 1023.

(29) Bleaney, B.; Bowers, K. D. *Proc. R. Soc. London* **1952**, *A214*, 451.

TABLE 3. Experimental Singlet−Triplet Splitting, T_{S-T}, of the Various Diradicals Based on IN and NN

	T_{S-T} (K)	note[b]
IN-*2p*-IN	−9.7[a]	BB
IN-*3p*-IN	−3.2	BB
X = Y = OC_{12}		
IN-*5p*-IN	−0.002	HFS
X = Y = OC_{14}		
IN-*pmp*-IN	−4.7[a]	BB
	−6.5	
IN-*pm*$_s$p-IN	−2.6	BB
X = CH_3; Y = OC_{12}		
IN-*pm*$_s$p-IN	−1.3	BB
X = H; Y = NO_2		
IN-*pm*-IN	>hfcc	*c*
NN-*pm*-NN	>hfcc	*c*
NN-*om*-NN	>hfcc	*c*

[a] Sample diluted in a polymer matrix, as obtained after lyophilization. [b] BB: Bleaney−Bowers model. HFS from the intermediate exchange limit deduced from the EPR spectra. hfcc: hyperfine coupling constant (see footnote c). [c] The value of the coupling is larger than the hfcc as observed on the EPR spectra in fluid solution (strong exchange limit). $|J/k|$ is in the range [10^{-3}, 10^{-1}] K, but the GS could not be determined.

hyperfine pattern in fluid solution, as expected within the strong exchange limit as discussed above. The Curie plots of the EPR susceptibility of frozen solutions yield oscillating values around the null ST splitting. Therefore, the magnetic GS of these compounds cannot be determined from these data. It is worth mentioning that within triradicals involving a similar topology, i.e., including the ***-2p-*** MCU, with ***pm*** connectivity, the triplet GS was observed with a through-bond exchange coupling between **IN** radicals of the order of 1 K or less.[6c,d]

The singlet GS found in the **IN-*pm*$_s$*p*-IN** derivatives does not agree with a simple application of the topological rules. This may be due to torsion of the radical fragments with respect to the conjugated MCU, as considered in previous observations of a singlet GS in *m*-phenylene-based diradicals.[4] However, there is no steric hindrance in the present case; moreover, the bis-**IN** *m*-phenylene based diradical has been shown to exhibit the triplet GS.[6b] The observed trends show that there is an effect of donor or acceptor substituent onto the phenyl ring, as recently reported in bis(semiquinone) diradical derivatives.[5e] This suggests the role of the excited electronic states in the magnetic properties of these diradicals.[30] Such a mechanism has already been considered in pyridinium-based diradicals with the meta topology,[31] as well as in the theoretical work (part 2) related to the present work. The nature of the magnetic GS of such compounds (S or T) depends on the degree of configuration interaction (CI) at which the calculations are performed.

For all linear derivatives the singlet GS is found as expected, the most interesting fact being as already discussed, the still operating through-bond spin−spin coupling within **IN-*5p*-IN**. The estimation of the ST gap for other singlet GS linear bis-**IN** diradical derivatives having short distances through the MCU between the **IN** radicals has been previously reported.[32,33] Reported values of T_{ST} are −289 K for Ullman's bis-**IN** diradical[32a,33] and −106 K for bis-**IN** diradical connected through a pyrimidinyl ring, bis-**IN-Pym**.[32b] The molecular conformation is quite different within these different compounds. For instance, the direct through-space magnetic interaction takes place in the Ullman's diradical. Experimentally, as depicted in the crystal packing, the molecular conformation is such as the twist angle between the two **IN** moieties is 55°.[32a] The calculations of the ST gap vs dihedral angle between the **IN** fragments[34] show that close to the planar conformation in the cis-conformer Ullman's bis-**IN** would have T_{ST} as high as ca. −2400 K, i.e., including strong through-space interaction. It would be ca. −200 K in the trans conformer with little through-space interaction. For bis-**IN-Pym**, the **IN** rings are twisted by 65°.[32b] A perfect planar conformation is observed for the whole molecule including the **IN** terminal radicals within the **IN-*3p*-IN** molecule.[11a,b] If this planar geometry is considered to be retained for the isolated molecule in solution, it may be considered that the phenylene-ethynylene MCU yields a rather weak exchange coupling, although propagating the exchange at long distances. This probably explains the failures for observing a significant magnetic coupling within poly(phenylene-ethynylene) polyradical derivatives as previously mentioned.[9a−c] A crude analysis of the decay of the ST gap within the **IN-*xp*-IN** derivatives yields T^0_{ST} = (173 ±22) K; d_0 = (5.2 ±0.3) Å within an empirical expression

$$T_{ST} = T^0_{ST} \exp(-d/d_0)$$

where d is the distance between the **IN** terminal fragments bearing the spin density.

Conclusion

The combination of *m*-phenylene topology together with the ethynyl triple bond has been shown to lead to *weak magnetic coupling* between the interconnected radical spins within diradicals and/or polyradical polymers.[10c−h] Related to such previous works on polyradical polymers, the present study reports on the design and synthesis of model diradicals based either on the *m*-phenylene topology or on the *p*-phenylene linear systems making use of the phenylene-ethynylene conjugated MCU.

The obtained results allow considering experimentally various effects on the intramolecular magnetic coupling in such diradicals. The singlet ground-state evidenced in the *m*-phenylene series, as well as the substituent effects, call for the theoretical investigation of these effects. The calculations must deal with the molecular conformation as already considered in various works, but also on the effects of the higher lying electronic states.

The lengthening of the MCU within a series of linear *p*-phenylene-ethynylene bis-imino radicals leads to the

(30) Mitani, M.; Yamaki, D.; Kitagawa, Y.; Yoshioka, Y.; Yamaguchi, K. *J. Chem. Phys.* **2000**, *113*, 10486.
(31) West, A. P., Jr.; Scott, Silverman, S. K.; Dougherty, D. A. *J. Am. Chem. Soc.* **1996**, *118*, 1452.
(32) (a) Alies, F.; Luneau, D.; Laugier, J.; Rey, P. *J. Phys. Chem.* **1993**, *97*, 2922. (b) Oshio, H.; Yaginuma, T.; Ito, T. *Inorg. Chem.* **1999**, *38*, 2750.
(33) Ullman, E. F.; Boocock, D. G. B. *J. Chem. Soc., Chem. Commun.* **1969**, 1161.
(34) Castell, O.; Caballol, R.; Subra, R.; Grand, A. *J. Phys. Chem.* **1995**, *99*, 154.

interesting fact that such a MCU is able to bridge magnetically two radical spins at very long distances. The negative fact is that the strength of the magnetic exchange coupling is weaker through phenylene-ethynylene than through phenylene-vinylidene oligomers. However, it is suggested that such a rigid rod conjugated connector may be of valuable interest in the design of magnetic networks within a supramolecular strategy. Moreover, the interest of such oligomer conjugated fragment has been successfully explored in photochemistry.[35]

Experimental Section

EPR Spectroscopy and Magnetic Measurements. EPR spectra were recorded with an X-band spectrometer operating at 9.5−9.9 GHz provided with a rectangular TE_{102} cavity, a NMR gaussmeter, a frequency meter, a power meter, and a continuous flow helium cryostat (3.8−300 K) for variable temperature. The temperature was independently checked by a gold−iron chromel thermocouple. Spin susceptibility χ_{EPR} was obtained by double integration of the EPR signal and compared with a calibrating sample. The microwave saturation effects have been considered by recording the EPR spectra at various attenuations of the microwave power, typically 30, 40, and 50 dB. Such a procedure has been especially followed at low temperature, where the saturation effects are known to be the strongest within diradicals/polyradicals. The microwave power supply is a Gunn diode with a maximum output of ca. 200 mW. At increasing microwave power, the lack of a departure from linear increase of the peak-to-peak amplitude of the EPR signal is considered to discard the saturation effects. It has been observed that at high temperature (above 50 K) a microwave attenuation of 40 dB was not distorting the EPR signal, whereas at lower temperature (down to 4 K) an attenuation of 50 dB was required. Since the $\Delta M_S = 1$ signal was the only one observable, its intensity was large enough so as to allow most measurements to be performed at 50 dB over a broad range of temperatures.

In the case of the **IN-*pmp*-IN**, the temperature dependence of the EPR signal has been recorded over the whole available range (4−100 K) and at three different microwave powers, as depicted by Rajca.[36] It was of great interest to confirm that this compound exhibits the singlet GS. The singlet GS is well established. We do notice that saturation effects would result in a decrease of the EPR line intensity, hence favoring an apparent singlet GS. However, a much larger apparent ST gap would be guessed as well, as depicted in the supplied Supporting Information. Moreover, a single Bleaney−Bowers law is no longer obeyed in the cases of line distortion by saturation effects.

In the case of the **IN-*2p*-IN**, the ST splitting has been determined for a diluted solution (1.5×10^{-4} mol^{-1}) within a polystyrene matrix as obtained by lyophilization.

The static magnetic properties of most powder compounds were measured on a SQUID susceptometer in the temperature range 2−100 K within a constant magnetic field in the range 0.1−0.5 T. The raw data were corrected from diamagnetic contributions of the sample holder, as well as from molecular diamagnetic contribution estimated by Pascal tables. These studies allow checking the reliability of the EPR spin calibration and the possibility of intermolecular ferro- or antiferromagnetic interactions.

Other Instrumentations. ^{1}H NMR spectra were recorded in $CDCl_3$ or DMSO at 200 MHz with a spectrometer operating at 200 MHz at room temperature. Melting points were measured with a dedicated apparatus or by differential scanning calorimetry at a heating rate of 10 °C/min. The ultraviolet and visible absorption spectra were measured with a conventional spectrophotometer. IR measurements were performed on KBr pellets. Raman spectra were recorded in solution (CD_2Cl_2/xylene, 1/1) with a 514 nm exciting wavelength from an argon laser.

Materials. Preparation of the 1,4-dibromo-2,5-bis(dodecanoxy)benzene and the 1,4-dibromo-2,5-bis(tetradecanoxy)benzene was already described in a previous paper.[13]

The following chemical reactives, 2-nitropropane, bromine, 4-bromobenzaldehyde, 4-bromoaniline, trimethylsilylacetylene (TMSA), palladium chloride ($PdCl_2$), triphenylphosphine (TPP), tetrabutylamonium fluoride 1.1 M in THF (TBAF), copper(II) acetate ($Cu(OAc)_2$), manganese dioxide (MnO_2), methyliodide (CH_3I), sodium nitrite ($NaNO_2$), diethylamine (Et_2N), and dichloromethane (CH_2Cl_2), were all of HPLC grade. All the chemical materials were used without further purification.

Hereafter, melting point ranges are reported for solid-state compounds.

2,3-Bis(hydroxyamino)-2,3-dimethylbutane (2). In a cooled (0 °C) solution of 40.6 g (0.76 mol) of ammonium chloride in water−methanol (400 mL + 400 mL) was suspended 70.5 g (0.4 mol) of 2,3-dimethyl-2,3-dinitrobutane. The mixture was kept below 15 °C with vigorous stirring during very slow addition (3 h) of 105 g zinc powder (1.6 mol). After addition, the stirring was continued for 3 h, and the temperature was allowed to rise 20 °C. The mixture was then filtered, and the separated cake of zinc oxide was washed with water (3 × 100 mL). The washings was acidified at pH 2 (140 mL, HCl 6 N) and evaporated under reduced pressure. Powdered anhydrous potassium carbonate (200 g) was then slowly added to the residual pale-yellow syrup to obtain a homogeneous white powder. From this, **2** was extracted with dichloromethane (400 mL) using a Soxhlet apparatus for 2 days. Compound **2** directly was crystallized in dichloromethane and filtered off to yield 33.4 g of white crystals. Yield: 57%. Mp: 161 °C. ^{1}H NMR (DMSO-d_6): δ 6.93 (s, 2H, −OH); 5.37 (s, 2H, −NH−); 0.97 (s, 12H, $-CH_3$). Anal. Calcd for $C_6H_{16}O_2N_2$: C, 48.64; H, 10.81; N, 18.91; O, 21.62. Found: C, 48.54;H, 10.88; N, 18.95; O, 21.60.

4-Trimethylsilylethynylbenzaldehyde (3). A deaerated solution of 4-bromobenzaldehyde (5 g, 25 mmol), TPP (0.328 g, 1.25 mmol), $PdCl_2$ (45 mg, 0.25 mmol), and $CuOAc_2$ (50 mg, 0.25 mmol) in 60 mL of anhydrous triethylamine was treated with TMSA (5.5 mL, 38 mmol). The mixture was heated at reflux for 6 h. After cooling, the precipitated triethylamine hydrobromide was filtered off (4.8 g, 98%), and the solvent was evaporated. The crude material was purified on a silica gel column using CH_2Cl_2/pentane, 1/3, as eluent to give 5.28 g of the silylated aldehyde **3**. Yield: 97%. Mp: 70 °C. ^{1}H NMR ($CDCl_3$): δ 8.7 (s, 1H, −CHO); 7.7 (dd, 4H, −PhH); 0.27 (s, 9H, $-SiCH_3$). Anal. Calcd for $C_{12}H_{14}SiO$: C, 71.28; H, 6.93; Si, 13.86; O, 7.92. Found: C, 71.30; H, 7.02; Si, 13.93; O, 7.83.

4-Ethynylbenzaldehyde (4). Compound **3** (5 g, 25 mmol) was treated with 0.35 g of K_2CO_3 (2.5 mmol, 10% mol) in 30 mL of MeOH at 25 °C for 2 h. The solvent was removed, and 50 mL of CH_2Cl_2 was added. The solution was washed with aqueous sodium bicarbonate, dried over Na_2SO_4, and concentrated to yield 3.1 g of a yellow solid. Yield: 96%. Mp: 87 °C. ^{1}H NMR ($CDCl_3$): δ 8.58 (s, 1H, −CHO); 7.87 (dd, 4H, −PhH); 3.3 (s, 1H, −C≡CH). Anal. Calcd: C, 83.07; H, 4.61; O, 12.30. Found: C, 82.93; H, 4.65; O, 12.39.

1,3-Dihydroxy-2-(4-bromophenyl)-4,4,5,5-tetramethyl-2-imidazoline (5). A mixture of 4-bromobenzaldehyde (1.85 g, 10 mmol) and 2,3-bis(hydroxylamino)-2,3-dimethylbutane (**2**) (1.34 g, 9.09 mmol) in 20 mL of MeOH was stirred under gentle reflux for 24 h. Addition of 5 mL of pentane and concentration of the mother liquor give a precipitate. Filtration yielded 1.85 g (65%) of the white hydrido adduct **5**. Mp: 205 °C. ^{1}H NMR (DMSO-d_6): δ 7.8 (s, 2H, −OH); 7.46 (dd, 4H, −PhH); 4.47 (s, 1H, $-HC_5$); 1.06 (s, 6H, $-CH_3$); 1.02(s, 6H,

(35) Hissler, M.; El-ghayoury, A.; Harriman, A.; Ziessel, R. *Angew. Chem., Int. Ed.* **1998**, *37*, 1717.

(36) Rajca, A.; Lu, K.; Rajca, S.; Ross, C. R., II. *Chem. Commun.* **1999**, 1249.

$-CH_3$) Anal. Calcd for $C_{13}H_{19}O_2N_2Br$: C, 49.52; H, 6.03; N, 8.88; O, 10.16. Found: C, 49.45; H, 5.99; N, 8.92; O, 10.18.

1,3-Dihydroxy-2-(p-ethynylphenyl)-4,4,5,5-tetramethyl-2-imidazoline (6). The procedure used to obtain **5** was followed with 0.966 g of ethynylbenzaldehyde (**4**) and 1 g of bis(hydroxylamine) (**2**) to give 1.37 g of the hydrido adduct **6**. Yield: 78%. Mp: 211 °C. ^{1}H NMR (DMSO-d_6): δ 7.8 (s, 2H, $-$OH); 7.45 (dd, 4H, $-$PhH); 4.49 (s, 1H, $-HC_5$); 4.13 (s, 1H, $-C\equiv CH$); 1.06(s, 6H, $-CH_3$); 1.02(s, 6H, $-CH_3$). Anal. Calcd for $C_{15}H_{20}O_2N_2$: C, 69.23; H, 7.69; N, 10.77; O, 12.30. Found: C, 68.95; H, 7.56; N, 10.66; O, 12.35.

Dimer IN-*2p*-IN (7). The procedure used to obtain **3** was followed with **5** (0.44 g, 1.39 mmol), **6** (0.363 g, 1.39 mmol), 25 mg of TPP, 4 mg of $PdCl_2$, 5 mg of $CuOAc_2$, and 30 mL of triethylamine. The crude material was purified on a silica gel column using CH_2Cl_2/EtOH, 9/1, as eluent to give 0.5 g of the yellow intermediate **7′**. Yield: 73%. ^{1}H NMR ($CDCl_3$): δ 8.15 and 7.55 (dd, 8H, $-$PhH); 1.35 (s, 12H, $-CH_3$); 1.30 (s, 12H, $-CH_3$). Oxidation: A solution of (**7′**) (100 mg, 0.22 mmol) in 10 mL of CH_2Cl_2 was stirred at room temperature during 2 h with MnO_2 (190 mg, 10 eq). After filtration, the dark red solution was concentrated, and the crude material was purified by preparative chromatography (eluent: CH_2Cl_2/EtOH 9.5/0.5). Recrystallization in hexane/CH_2Cl_2 yields 95 mg (96%) of red crystals **(7)**. Mp: 180 °C. Anal. Calcd for $C_{14}H_{32}O_2N_4$: C, 73.68; H, 7.45; O, 7.01; N, 12.28. Found: C, 73.78; H, 7.05; O, 7.25; N, 12.30.

Trimer IN-*3p*-IN (8). The procedure used to obtain **3** was followed with 1,4-dibromo-2,5-bis(dodecanoxy)benzene (1 g, 1 equiv), **6** (0.950 g, 2.2 equiv), 43 mg of TPP, 6 mg of $PdCl_2$, 7 mg of $CuOAc_2$, and 50 mL of triethylamine. The crude material was purified on a silica gel column using CH_2Cl_2/EtOH, 9/1, as eluent to give 1.12 g of the yellow intermediate **8′**. Yield: 73%. ^{1}H NMR ($CDCl_3$): δ 8.3 and 7.55 (dd, 8H, $-PhH_1$); 7 (s, 2H, $-PhOC_{12}$); 4.05 (t, 4H, $-OCH_2$ α ether); 1.86 (q, 4H, $-CH_2-$ β ether); 1.39 (s, 12H, $-CH_3$); 1.33 (s, 12H, $-CH_3$); 1.25 (s, 36H, $-CH_2-$ δ); 0.86 (t, 6H, $-CH_3$t). Oxidation: The procedure to obtain **7** was followed with **8′** (200 mg) and 10 equivalent of MnO_2 in 10 mL of CH_2Cl_2. Recrystallization in hexane/CH_2Cl_2 yields 170 mg (85%) of red crystals (**8**). Mp: 102 °C. Anal. Calcd for $C_{60}H_{84}O_4N_4$: C, 77.92; H, 9.09; O, 6.92; N, 6.06. Found: C, 77.85; H, 9.23; O, 6.87; N, 5.92.

1-(4-Bromophenyl)-3,3-diethyltriazene (9). 4-Bromoaniline (10.32 g, 60 mmol), 7.5 mL of chlorhydrique acid, and 9 mL of water were charged and stirred in a vessel frozen (0 °C) with an ice$-$salt bath. A cold solution of sodium nitrite (4.54 g, 66 mmol) in 7.5 mL of water was slowly added. The mixture was stirred for 30 min, keeping the temperature under 0 °C. The diazonium solution was then slowly added to a frozen mixture of potassium carbonate (12.44 g, 90 mmol) and diethylamine (6.58 g, 90 mmol) in 120 mL of water and stirred for 30 min, while the temperature was allowed to increase to room temperature. The mixture was extracted with ether. The organic fraction was washed with water, dried over Na_2SO_4, and evaporated. The crude material was purified by silica gel chromatography using heptane/CH_2Cl_2, 2/1, as eluent to give 14 g pure triazene **9** (yellow liquid). Yield: 91%. ^{1}H NMR ($CDCl_3$): δ 7.37 (dd, 4H, $-$PhH); 3.76 (q, 4H, $-CH_2$-); 1.27 (t, 6H, $-CH_3$).

1-(4-Trimethylsilylethynylphenyl)-3,3-diethyltriazene (10). The procedure used to obtain **3** was followed with **9** (8 g, 1 equiv), 3.82 mL (1.5 equiv) of TMSA, 0.2 g (5% mol) of TPP, 28 mg (1% mol) of $PdCl_2$, 31 mg (1% mol) of $CuOAc_2$, and 50 mL of triethylamine. The crude material was purified on a silica gel column using CH_2Cl_2/pentane, 1/2, as eluent to give 6.5 g of orange liquid (**10**). Yield: 76%. ^{1}H NMR ($CDCl_3$): δ 7.42 (dd, 4H, $-$PhH); 3.77 (q, 4H, $-CH_2-$); 1.27 (t, 6H, $-CH_3$); 0.25 (s, 9H, $-SiCH_3$).

4-Iodotrimethylsilylethynylbenzene (11). Compound **10** (5 g) was taken up in freshly distilled methyl iodide (10 mL). The solution was degassed and placed under nitrogen, and the tube, sealed (**thick walled tube; take care to the overpressure of nitrogen**). After heating for 24 h at 115 °C, the reaction mixture was poured into 50 mL of pentane. The precipitate was filtered off and separated by chromatography through a silica gel column using CH_2Cl_2/pentane, 1/4, as eluent to give 4.85 g of the iodide derivative **11**.Yield: 97%. ^{1}H NMR ($CDCl_3$): δ 7.64 and 7.19 (dd, 4H, $-$PhH); 0.25 (s, 9H, $-SiCH_3$).

Dimer Intermediate 12. The procedure used to obtain **3** was followed with **11** (3 g, 10 mmol), **6** (2.3 g, 0.9 mmol), 118 mg of TPP, 16 mg of $PdCl_2$, 18 mg of $CuOAc_2$, and 100 mL of triethylamine. The crude material was purified on a silica gel column using CH_2Cl_2/EtOH, 9.5/0.5, as eluent to give 3.5 g of the yellow intermediate **12′**. Yield: 95%. ^{1}H NMR ($CDCl_3$): δ 8.24 and 7.54 (dd, 4H, $-Ph_2H$); 7.47 (s, 4H, $-Ph_1H$); 1.36 (s, 6H, $-CH_3$); 1.34 (s, 6H, $-CH_3$); 0.25 (s, 9H, $-SiCH_3$). Deprotection: **12′** (3 g, 7 mmol) was dissolved in 10 mL of THF, and TBAF (0.23 g, 0.9 mmol) was slowly added leading to a black solution. After 10 min, the reaction was filtered through a plug of silica gel. The solvent was evaporated and the crude product was separated by chromatography through a silica gel column using CH_2Cl_2/éthanol, 9.5/0.5 as eluent, to give 2.1 g of the yellow deprotected dimer (**12**). Yield: 85%. ^{1}H NMR ($CDCl_3$): δ 8.25 and 7.54 (dd, 4H, $-Ph_2H$); 7.47 (s, 4H, $-Ph_1H$); 3.2 (s, 1H, $-C\equiv CH$); 1.36 (s, 6H, $-CH_3$); 1.34 (s, 6H, $-CH_3$).

Pentamer IN-*5p*-IN (13). The procedure used to obtain **3** was followed with 1,4-dibromo-2.5-bis(tetradecanoxy)benzene (1.5 g, 2.3 mmol), **12** (1.78 g, 5.3 mmol), 60 mg (5% mol) of TPP, 8 mg (1% mol) of $PdCl_2$, 9 mg (1% mol) of $CuOAc_2$, and 50 mL of triethylamine. The crude material was purified on a silica gel column using CH_2Cl_2/ethanol, 9.5/0.5, as eluent, to give 1.4 g of yellow powder **(13′)**. Yield: 53%. ^{1}H NMR ($CDCl_3$): δ 8.29 and 7.54 (dd, 8H, $-Ph_2H$); 7.50 (s, 8H, $-Ph_1H$); 7,00 (s, 2H, $PhOC_{12}$); 4.03 (t, 4H, $-OCH_2-$ α ether); 1.86 (q, 4H, $-CH_2-$ β ether); 1.39 (s, 12H, $-CH_3$); 1.33 (s, 12H, $-CH_3$); 1.25 (s, 44H, $-CH_2-$ δ); 0.87 (t, 6H, $-CH_3$ t). Anal. Calcd for $C_{80}H_{102}O_4N_4$: C, 81.21; H, 8.63; O, 5.41; N, 4.73. Found: C, 79.27; H, 8.60; O, 5.50; N, 4.52. Oxidation: A solution of **13′** (150 mg, 1 equiv) in 10 mL of CH_2Cl_2 was stirred at room temperature during 2 h with MnO_2 (20 equiv). After filtration, the dark red solution was concentrated, and the crude material was purified by preparative chromatography (eluent: CH_2Cl_2/EtOH 9.5/0.5). Recrystallization in heptane/CH_2Cl_2 yields 133 mg of red crystals (**13**). Yield: 89%. Mp: 169 °C. Anal. Calcd for $C_{80}H_{100}O_4N_4$: C, 81.35; H, 8.47; O, 5.42; N, 4.74. Found: C, 80.62; H, 8.43; O, 5.46; N, 4.53.

Trimer IN-*pmp*-IN (X = H, Y = H) (14). The procedure used to obtain **3** was followed with 1,3-dibromobenzene (0.5 g, 1 equiv), **6** (1.21 g, 2.2 equiv), 61 mg (5% mol) of TPP, 8.5 mg (1% mol) of $PdCl_2$, 9.5 mg (1% mol) of $CuOAc_2$, and 40 mL of triethylamine. The crude material was purified on a silica gel column using CH_2Cl_2/ethanol, 9/1 as eluent, to give 0.83 g of yellow powder (**14′**). Yield: 71%. ^{1}H NMR (DMSO): δ 8.04 and 7.68 (dd, 8H, $-Ph_1H$); 7.79 (t, 1H, $-Ph_2H_B$); 7,65 (dd, 2H, Ph_2H_A); 7.55 (t, 1H, Ph_2H_C), 1.18 (s, 12H, $-CH_3$); 1.16 (s, 12H, $-CH_3$). Oxidation: A solution of **14′** (400 mg, 1 equiv) in 10 mL of CH_2Cl_2 was stirred at room temperature during 2 h with MnO_2 (20 equiv). After filtration, the dark red solution was concentrated, and the crude material was purified by preparative chromatography (eluent: CH_2Cl_2/EtOH 9.5/0.5). Recrystallization in heptane/CH_2Cl_2 yields 360 mg of red crystals (**14**). Yield: 90%. Mp: 115 °C. Anal. Calcd for $C_{36}H_{36}O_2N_2$: C, 77.69; H, 6.47; O, 5.75; N, 10.07. Found: C, 77.48; H, 6.46; O, 5.77; N, 10.28.

Trimer IN-*pm*$_s$*p*-IN (X = CH_3, Y OC_{12}) (15). The procedure used to obtain **3** was followed with 1,3-dibromo-2-methyl-5-dodecanoxybenzene (0.646 g, 1 equiv), **6** (0.852 g, 2.2 equiv), 43 mg (5% mol) of TPP, 6 mg (1% mol) of $PdCl_2$, 6.5 mg (1% mol) of $CuOAc_2$, and 40 mL of triethylamine. The crude material was purified on a silica gel column using CH_2Cl_2/ethanol, 9/1 as eluent, to give 0.765 g of yellow powder (**15′**). Yield: 68%. ^{1}H NMR ($CDCl_3$): δ 8.29 and 7.60 (dd, 8H, $-Ph_1H$); 6.95 (s, 2H, $-Ph_2H$); 3.93 (t, 2H, $-OCH_2-$ α ether);

2.54 (s, 3H, −PhCH$_3$); 1.72 (q, 2H, −CH$_2$− β ether); 1.40 (s, 12H, −CH$_3$); 1.34 (s, 12H, −CH$_3$); 1.27 (s, 18H, −CH$_2$- δ); 0.88 (t, 3H, −CH$_3$t). Oxidation: A solution of **15′** (150 mg, 1 equiv) in 10 mL of CH_2Cl_2 was stirred at room temperature during 2 h with MnO_2 (20 equiv). After filtration, the dark red solution was concentrated, and the crude material was purified by preparative chromatography (eluent CH_2Cl_2/EtOH 9.8/0.2). Recrystallization in heptane/CH_2Cl_2 yields 130 mg of red crystals (**15**). Yield: 87%. Mp: 125 °C dec. Anal. Calcd for $C_{49}H_{62}O_3N_4$: C, 77.98; H, 8.22; O, 6.36; N, 7.43. Found: C, 77.56; H, 9.18; O, 6.62; N, 7.60.

Trimer IN-*pm*$_s$*p*-IN (X = CH$_3$, Y = OCH$_3$) (15B). The procedure used to obtain **3** was followed with 1,3-dibromo-2-methyl-5-methoxybenzene (0.972 g, 1.49 mmol, 1 equiv), **6** (1.98 g g, 2.2 equiv), 100 mg (5% mol) of TPP, 13.5 mg (1% mol) of $PdCl_2$, 15.5 mg (1% mol) of $CuOAc_2$, and 40 mL of triethylamine. After purification, 0.765 g of yellow powder (**15B′**) was obtained. Yield: 67%. ^{1}H NMR ($CDCl_3$): δ 8.20 and 7.36 (dd, 8H, −Ph$_1$H); 6.88 (s, 2H, −Ph$_2$H); 3.71 (s, 3H, −OCH$_3$); 2.51 (s, 3H, −PhCH$_3$); 1.38 (s, 12H, −CH$_3$); 1.34 (s, 12H, −CH$_3$); Oxidation: reaction by the same procedure as for **15** on 200 mg of **15B′**. Recrystallization, 175 mg of red crystals (**15B**). Yield: 87%. Mp 130 °C dec. Anal. Calcd for $C_{38}H_{40}O_3N_4$: C, 75.97; H, 6.71; O, 7.99; N, 9.33. Found: C, 76.37; H, 6.70; O, 8.00; N, 8.91.

3,5-Dibromonitrobenzene (16). A 4.4 mL (2 equiv) portion of hydrochloric acid was slowly added to a heated mixture of 2,6-dibromo-4-nitroaniline (10.36 g, 1 equiv), 17 mL of benzene, and 50 mL of ethanol. The mixture was heated under reflux, and then 6 g (1.6 equiv) of sodium nitrite was added. After 12 h, the mixture was cooled and extracted with ether. The organic fraction was washed with water, dried over Na_2SO_4, and evaporated to give 7.86 g of powder (**16**). Yield: 80%. Mp: 95 °C. ^{1}H NMR ($CDCl_3$): δ 8.33 (d, 2H, −PhH); 8 (t, 1H, −PhH). Anal. Calcd for $C_6H_3O_2N_1Br_2$: C, 25.62; H, 1.06; O, 11.38; N,4.98. Found: C, 25.65; H, 1.10; O, 11.34; N, 4.98.

Trimer IN-*pm*$_s$*p*-IN (X = H, Y = NO$_2$) (17). The procedure used to obtain **3** was followed with 1,3-dibromo-2-methyl-5-dodecanoxybenzene (**16**) (0.5 g, 1 equiv), **6** (1.02 g, 2.2 equiv), 51 mg (5% mol) of TPP, 7 mg (1% mol) of $PdCl_2$, 7.5 mg (1% mol) of $CuOAc_2$, and 40 mL of triethylamine. The crude material was purified on a silica gel column using CH_2Cl_2/ethanol, 8/2 as eluent, to give 0.8 g of yellow powder **(17′)**. Yield: 75%. ^{1}H NMR ($CDCl_3$): δ 8.40 (d, 2H, −Ph$_2$H$_A$); 8.22 (t, 1H, −Ph$_2$H$_B$); 8.06 and 7.73 (dd, 8H, −Ph$_1$H); 1.19 (s, 12H, −CH$_3$); 1.17 (s, 12H, −CH$_3$). Oxidation: A solution of **17′** (100 mg, 1 equiv) in 10 mL of CH_2Cl_2 was stirred at room temperature during 2 h with MnO_2 (20 eq). After filtration, the dark red solution was concentrated, and the crude material was purified by preparative chromatography (eluent: CH_2Cl_2/EtOH 9/1). Recrystallization in heptane/CH_2Cl_2 yields 95 mg of red crystals (**17**). Yield: 85%. Mp: 200 °C. Anal. Calcd for $C_{36}H_{35}O_4N_5$: C, 71.88; H, 5.82; O, 10.64; N, 11.64. Found: C, 72.24; H, 5.80; O, 10.30; N, 11.65.

1-(4-Formylphenyl)-2-(3-formylphenyl)ethyne (18). The procedure used to obtain **3** was followed with 3-ethynylbenzaldehyde (1 g, 1 equiv), 4-bromobenzaldehyde (1.42 g, 1 equiv), 100 mg of TPP, 14 mg of $PdCl_2$, 15 mg of $CuOAc_2$, and 30 mL of triethylamine. The crude material was purified on a silica gel column using CH_2Cl_2/pentane, 7/3 as eluent, to give 1.6 g of the yellow dialdehyde (**18**). Yield: 89%. ^{1}H NMR ($CDCl_3$): δ 8.54 (s, 2H, −CHO); 8.10 (t, 1H, −Ph$_2$H); 7.9 and 7.71 (dd, 4H, −Ph$_1$H); 7.84 and 7.80 (dt, 2H, −Ph$_2$H); 7.58 (t, 1H, −Ph$_2$H). Anal. Calcd for $C_{16}H_{10}O_2$: C, 82.05; H, 4.27. Found: C, 81.64; H, 4.20.

Dimer NN-*pm*-NN (19). The procedure used to obtain **5** was followed with **18** (0.5 g, 1 equiv) and bis(hydroxylamine) (**2**) (0.695 g, 2.2 equiv) to give 0.8 g of the hydrido adduct (**19′**). Yield: 76%. ^{1}H NMR (DMSO-d_6): δ 7.84 and 7.45 (dd, 4H, −Ph$_1$H); 7.65 (t, 1H, −Ph$_2$H); 7.51 (s, 4H, −OH); 7.5 to 7.36 (m, 3H, −Ph$_2$H and −Ph$_2$H); 4.52 (s, 2H, −HC5); 1.07 (s, 12H, −CH3); 1.04 (s, 12H, −CH$_3$). Oxidation: A solution of **19′** (100 mg, 1 equiv) in 10 mL of CH_2Cl_2 was stirred at room temperature during 2 h with MnO_2 (20 equiv). After filtration, the dark blue solution was concentrated, and the crude material was purified by preparative chromatography (eluent: CH_2Cl_2/EtOH 9/1). Recrystallization in heptane/CH_2Cl_2 yields 70 mg of blue crystals (**19**). Yield: 71%. Mp: 196 °C. Anal. Calcd for $C_{28}H_{32}O_4N_4$: C, 68.85; H, 6.56; O, 13.11; N, 11.47. Found: C, 68.48; H, 6.55; O, 13.50; N, 10.96.

1-(4-Formylphenyl)-2-(2-formylphenyl)ethyne (20). The procedure used to obtain **3** was followed with 3-ethynylbenzaldehyde (1 g, 1 equiv), 2-bromobenzaldehyde (1.42 g, 1 equiv), 100 mg of TPP, 14 mg of $PdCl_2$, 15 mg of $CuOAc_2$, and 30 mL of triethylamine. The crude material was purified on a silica gel column using CH_2Cl_2/pentane, 7/3, as an eluent to give 1.5 g of the yellow dialdehyde (**20**). Yield: 87%. ^{1}H NMR ($CDCl_3$): δ 10.65 (s, 1H, −CHO); 10.2 (s, 1H, −CHO); 8.15 (s, 1H, −PhH); 7.98 to 7.75 (m, 3H, −PhH); 7.72 and 7.45 (m, 4H, −PhH). Anal. Calcd for $C_{16}H_{10}O_2$: C, 82.05; H, 4.27; Found: C, 81.87; H, 4.28.

Dimer NN-*om*-NN (21). The procedure used to obtain **5** was followed with **20** (0.5 g, 1 equiv) and bis(hydroxylamine) (**2**) (0.695 g, 2.2 equiv) to give 0.4 g of the hydrido adduct (**21′**). Yield: 66%. ^{1}H NMR (DMSO-d_6): δ 7.80 (s, 2H, −OH$_2$); 7.72 to 7.68 (m, 2H, −PhH); 7.60 (s, 2H, −OH$_1$); 7.48 to 7.25 (m, 6H, −PhH); 4.49 (s, 2H, −HC5); 1.08 (s, 12H, −CH3); 1.06 (s, 6H, −CH3); 1.05 (s, 6H, −CH3). Oxidation: A solution of **21′** (100 mg, 1 equiv) in 10 mL of CH_2Cl_2 was stirred at room temperature during 2 h with MnO_2 (20 equiv). After filtration, the dark blue solution was concentrated, and the crude material was purified by preparative chromatography (eluent: CH_2Cl_2/EtOH 9/1). Recrystallization in heptane/CH_2Cl_2 yields 80 mg of blue crystals (**21**). Yield: 81%. Mp: 150 °C dec. Anal. Calcd for $C_{28}H_{32}O_4N_4$: C, 68.85; H, 6.56; O, 13.11; N, 11.47. Found: C, 68.94; H, 6.48; O, 13.08; N, 10.99.

Acknowledgment. We are grateful to Drs. A. Pham and J. Y. Bigot at IPCMS for the Raman measurements. Mr. M. Bernard is thanked for invaluable help in the setup of the EPR measurements at ICS. We express thanks to Dr. L. Catala, who prepared the lyophilized samples and performed complementary measurements on the compound **IN-*pmp*-IN**. Part of this work has been financially supported by an EU Program "Marie Curie Doctoral Training Site: Chemical Synthesis and Electron Paramagnetic Resonance of Molecular Magnets (Contract No. HPMT-2000-00083). V.V. was awarded a one-year fellowship within this EU program. Prof. J. Simon is acknowledged for his careful reading of the manuscript and for valuable comments. We thank Prof. A. Bieber and Prof. J.-J. André for interactive and constructive discussions while they were performing the pendant theoretical work of this contribution (Part 2, to be published separately).

Supporting Information Available: Spectral data (IR), EPR spin susceptibility (microwave power effects), and static susceptibility for polycrystalline samples (SQUID measurements). This material is available free of charge via the Internet at http://pubs.acs.org.

JO034723N